Proceedings of the Second International Workshop on EGS, 8.-12. August 2000, Tsukuba, Japan
KEK Proceedings 200-20, pp.11-22

Improvements of Low Energy Photon Transport for EGS5

Y. Namito, H. Hirayama and S. Ban

High Energy Accelerator Research Organization (KEK)
Oho, Tsukuba-shi, Ibaraki-ken, 305-0801, Japan

Abstract

We have implemented additional functions to EGS4 code [1]. We describe each modification of EGS4 after the 1st international EGS4 workshop [2]. The items are; i) L-X ray ii) Electron impact ionization, iii) Auger electron and iv) X ray and Auger from compound and mixture. Then, we describe two systematic comparison of improved EGS4 code and measurements, which were performed to verify the validity of the improvement. The comparison are "20-40 keV synchrotron radiation scattering experiment" and "Electron beam induced K-X ray intensity". Agreement of calculation and experiment were satisfying level in both comparisons.

1 Introduction

In the 1st international EGS4 workshop in 1997, we presented improvements of low energy photon transport of EGS4 code. The items of the improvements were,

- Linearly polarized photon scattering [3],
- Doppler broadening in Compton scattering [4],
- L-X ray [5],
- Electron impact ionization [6].

We continue an improvement of low energy photon transport of EGS4 code which will be integrated as part of EGS5 code. The new improvements are,

- Revision of L-X ray,
- Revision of Electron impact ionization,
- Auger electron,
- X ray/Auger from compound/mixture.

In Sec. 2, these new improvements are described.

Two systematic comparisons of measurements and EGS4 code were performed to verify the validity of the improvement. These comparisons were described in Sec 3. The first comparison is "20-40 keV synchrotron radiation scattering experiment". Targets are C, Cu, Ag, and Pb. Compton, Rayleigh, K-X, L-X rays are observed using Ge detectors. L-X rays from Gd sample were also measured.

The second comparison is "Electron beam induced K-X ray". Electron beam of 10-3000 keV incident normally on targets (Al,Ti,Cu,Ag and Au) and K-X ray intensity was calculated at 120° and 180°. Comparison of photon spectra from Cu and Sn target due to electron beam incident were also performed.

All the improvements until now are available as programs [7] and manuals [8, 9].

2 Improvements of Programs

2.1 L-X ray

2.1.1 Energy dependent L subshell cross sections

In 1996 version of L-X ray calculation [5], the ratio of L subshell photoelectric effect cross sections at the energy of L-edges was used and any energy dependence of the ratio was ignored. This introduced an error greater than negligible level. We implemented energy dependence of the ratio of L subshell photoelectric effect cross sections using Matese and Johnson's calculated L subshell photoelectric effect cross sections [10].

2.1.2 Emission rates library based on experiment values

In 1996 version of L-X ray calculation [5], we used Scofield's calculated K and L emission rates [11]. In the current version, we use Salem's experimental K and L emission rates [12]. EGS4 calculation using Salem's value gives better agreement with measurements comparing to calculation using Scofield's value.

2.1.3 Local extrapolation method (LEM)

To avoid possible underestimation of X rays near edge-energy two modifications were applied.

1. Improvement of piecewise linear fitting named 'Local extrapolation method'(LEM) to treat mean free path and branching ratio near to edge. [13]
2. Increasing the number of photon energy intervals from 200 to 1000.

2.2 EII

In 1999, we implemented EII into EGS4 code. [6] We updated EII calculation function so that it is ready to built up for EGS5. Here, following modifications were applied to EII calculation.

1. Common subroutine with photoelectric effect is used in K-X calculation.
2. EII of any element in compound and mixture is treated.

In the same time, the treatment of photoelectric effect related phenomena in EGS4 code was also changed. As a result of this, following points were also modified,

1. Fluorescent yield was updated from [14, 15] to [16, 17]. The ratio of currently used and previously used fluorescent yield is shown in Fig.1.
2. Possible underestimation of K_β is now avoided by means of LEM and increasing the number of photon energy intervals.
3. The number of the energy of K-X ray is increased from 4 to 10.

2.3 Auger electron

Auger electron calculation was added to EGS4 code. Data and method of calculation is described in [9].

Guadala et al measured electron spectra from Al and Ti target using monochronized synchrotron radiation photon at BNL. [18] Electron emitted to forward direction of 10° opening angle were measured with energy resolution of 3%. We simulated Guadala's experiment using the improved EGS4 code. As the photon energy was not measured, we adjusted incident photon energy from Compton recoil energy. Comparison of measurement and calculation is shown in Fig. 2. EGS4 underestimated Auger electron from Al sample. EGS4 reproduced Auger electron from Ti sample and Compton recoil electron from both the samples.

Table 1: Incident photon energy and linear polarization

Energy (keV)	40	30	20
Linear Polarization (P)	0.885	0.877	0.873

Table 2: Samples and their thickness

Sample	C	Cu	Ag	Pb
T (g/cm^2)	0.1325	1.79	0.525	0.568

2.4 X ray/Auger from compound/mixture.

We modified pegs4 program so that the ratio of photo electric effect cross sections of each element in compound and mixture is output as a function of photon energy. We also modified EGS4 program to read in this ratio and to use it to select element in photoelectric effect in compound and mixture. After the element is sampled in the calculation, either X ray or Auger electron from that element is followed. The detail of the calculation method is described in [9].

3 Systematic Comparison of Measurement and Calculation

3.1 Photon Beam Incident

We performed a mono-energy photon-scattering experiment at a BL-14C in a 2.5 GeV synchrotron light facility (PF). The experimental arrangement is shown in Fig.3. Photons from a vertical wiggler were used after being monochronized by a Si(1,1,1) double crystal monochrometer. A linearly polarized mono-energy photon beam was scattered by a sample located at point O with its normal vector $(-\frac{1}{2}, -\frac{1}{\sqrt{2}}, \frac{1}{2})$; the scattered photons were detected by two high-purity Ge detectors located at $\theta = 90^\circ$. Incident photon energies and linear polarization are shown in Table 1. Sample and their thickness are shown in Table 2. One Ge detector (Ge_2) was located in the plane of the incident polarization vector($\phi = 0^\circ$), and the other (Ge_1) in the plane perpendicular to it ($\phi = 90^\circ$). Samples were contained in a vacuum chamber, and vacuum pipes were placed between the vacuum chamber and the Ge detectors in order to reduce any scattering due to the air. Collimators of 5.01 mm aperture were placed in front of Ge detectors (C_1, C_2). The distance from the surface of the sample to the collimator was 420 mm. The opening angle of this collimator was 0.33° and the energy spread of a Compton-scattered photon due to this opening angle (without Doppler broadening) was negligibly small, 31eV for incident beam of 40 keV. The incident photon intensity was monitored in a free–air ionization chamber, which was calibrated using a calorimeter [19].

Two stage EGS4 calculation was performed. In the first stage, photon beam incident on the sample and emergent photons (A) are scored. In the second stage, energy deposition in Ge detector was calculated while using 'A' as a photon source.

Measured and calculated photon spectra are shown in Fig. 4. The spectrum by EGS4 calculation is smeared by Gaussian function of FWHM=0.3 keV to account for the resolution of Ge detector. The shape of Compton scattering, Rayleigh scattering, K-X ray and L-X ray peaks are well reproduced by the EGS4 calculation.

The ratio of measured and calculated peaks are shown in Fig. 5. In the L-X ray comparison, preliminary data of Gd sample are also shown. $|C/M - 1| \sim 0.03$ for Compton, 0.6 for Rayleigh, 0.04 for K-X and 0.15 for L-X.

Table 3: Geometric average of C/M of K-X ray yields. Gr and Ca means the calculation result using Gryziński's and Casnati's cross section, respectively.

Target	Al	Ti	Cu	Ag	Au	Av
EGS4	0.0027	0.023	0.053	0.31	0.85	0.061
EGS4+EII(Gr)	0.96	1.12	0.86	0.91	1.07	0.98
EGS4+EII(Ca)	1.16	1.40	1.18	1.11	1.16	1.21

3.2 Electron Beam Incident

We simulated following three measurements.

1. Dick et al performed a systematic measurement of K-X ray when electron beam of 10, 20, 40, 100, 200, 500, 1500 and 3000 keV hits target(Al, Ti, Cu, Ag and Au) normally. [20] K-X ray yield per incident electron was measured at $\theta = 120^\circ$ and 180°.

2. Acosta et al measured photon spectra emitted from Cu target at $\theta = 140^\circ$ using Si detector when an electron beam of 20 keV incident normally on the target [23].

3. Placious measured bremsstrahlung photons and K-X rays from Sn targets iat $\theta = 70^\circ$ and 140° for the normal incidence of 100 keV electrons [21, 22].

EGS4 calculation with and without the improvement to treat EII were performed. As a K-shell EII cross section, Gryziński's relativistic cross section [24] were used. All the comparisons were done in absolute, i.e. no normalization between the measurement and the calculation were done.

To simulate Acosta's experiment, two stage calculation was done. In the first stage, photons emerging from the target to θ=125-135° was scored (A). In the second stage, we calculated energy deposition in Si detector using "A" as a source. All the absorbing layers in Si detector were considered.

3.2.1 K-X ray yield

The calculated and measured K-X ray yields are shown in Fig. 1. The statistical error in the calculation is within 3% for EGS4+EII, 10% and 5% for EGS4 of Al and other targets, respectively. The geometric average of the ratio of the calculated K-X ray yield to the measured one is shown for each target in Table 1. Here, a result of EGS4+EII calculation using Casnati's EII cross section [25, 26] is also shown, whose agreement with measurement is worse comparing to the calculation using Gryziński's cross section.

The EGS4 calculation apparently becomes underestimated with decreasing Z of the target. C/M is only 0.0027 for Al, but C/M is 0.85 for Au. The degree of underestimation depends weakly on the electron incident energy and the scoring angle.

For Al, Ti, Cu and Ag sample, dominant contribution of K-X ray is EII. For Au sample, dominant contribution of K-X ray is photoelectric effect of bremsstrahlung photon.

3.2.2 Photon spectra from a Cu target

The calculated and measured photon spectra from Cu target are shown in Fig. 2. C/M=0.92, 0.83 and 0.85 for energy intervals of 1-7.6 (low energy bremsstrahlung), 7.6-9.2 (K-X) and 9.2-20 keV (high energy bremsstrahlung) when EII is considered in a calculation. When EII is ignored, C/M=0.07 in K-X region. Gauss smearing of FWHM=1.6 keV were applied to the EGS4 result to simulate energy resolution of the Si detector.

3.2.3 Photon spectra from a Sn target

The calculated and measured photon spectra from Sn target are shown in Fig. 3. C/M=0.74 and 0.88 at $\theta = 70^\circ$ and $\theta = 110^\circ$, respectively for energy intervals of 10.0-36.0 keV (K-X) when EII is considered in a calculation. When EII is ignored, C/M=0.52 and 0.67 at $\theta = 70^\circ$ and $\theta = 110^\circ$, respectively for energy region of 10.0-36.0 keV.

As NaI detector was used in this measurement, energy resolution is not good comparing to Acosta's measurement. Then, large amount of bremsstrahlung photon contributed to the counts in the K-X ray energy region. Gauss smearing of FWHM=8 keV were applied to the EGS4 result to simulate energy resolution of the NaI detector.

4 Discussion

4.1 Photon beam incident

4.1.1 Rayleigh scattering

As shown in Fig.5(b), measured and calculated intensity of Rayleigh scattered photon differs by factor of 1.5 or more. This is due to interference between Rayleigh scattered photons.

About C and Pb sample, $|M/C| - 1 < 0.15$. This means the effect of interference is small for these samples, The difference between that in horizontal and vertical directions are small. This means that the azimuth angle dependence is small. It may be possible to simulate interference of Rayleigh scattering from C and Pb sample by modifying the form factor of Rayleigh scattering in the same way as that of water [27].

4.1.2 L-X ray

M/C$\sim$1.07 and 0.85 for Gd and Ag. There are possible sources of errors both in experimental side and calculation side.

Measuring Ag L-X ray is more difficult comparing to other measurements because of its low energy (2.5-4 keV). The efficiency of Ge detectors change largely depending on energy and attenuation due to air and Kapton film is also evident. The measurement of Gd L-X ray is only preliminary and these data may be changed in the future measurement.

The error of L-shell fluorescent yields (Ω_{L_1}, Ω_{L_2} and Ω_{L_3}) are 30-20, 25-10 and 20-10% respectively for Ag, 15, 10-5 and 5% respectively for Gd. [16]

4.2 EII

Among 62 comparison between Dick's K-X ray yield measurement and EGS4 calculation, $|C/M-1|$ was within 0.15 for 41 cases. We guess the largest source of the discrepancy between measurement and calculation is the error in EII cross section.

In the comparison of Dick's measurement and EGS4 calculation, C/M=0.79 when electron energy=20 keV, target=Cu and $\theta = 120^\circ$. In the comparison of Acosta's measurement and EGS4 calculation, C/M=0.83. The close agreement of two C/M values suggest that both experiment values are consistent.

In the comparison of Acosta's measurement and EGS4 calculation, high energy part of bremsstrahlung photon was underestimated. Similar underestimation of bremsstrahlung at high photon energy side was also seen in the comparison of photon spectra from a Sn target. We guess these underestimation can be fixed by using better bremsstrahlung photon generation cross section.

5 Conclusion

Two systematic comparisons of measurements and EGS4 code were performed to verify the validity of the improvement. The first comparison is "20-40 keV synchrotron radiation scattering experiment". Targets are C, Cu, Ag, and Pb. Compton, Rayleigh, K-X, L-X rays are observed using Ge detectors. L-X rays from Gd sample were also measured. The agreement of EGS4 and the measurement was good both in the energy spectral shape and intensity: $|C/M-1| \sim 0.03$ for Compton, 0.6 for Rayleigh, 0.04 for K-X and 0.15 for L-X.

Systematic comparison of measured and calculated K-X ray yield from various target for electron beam of 0.01 to 3 MeV was performed without any normalization. General agreement between measurement and calculation show the validity of improved EGS4 code. For Al, Ti, Cu and Ag sample, dominant contribution of K-X ray is EII. For Au sample, dominant contribution of K-X ray is photoelectric effect of bremsstrahlung photon.

References

[1] W. R. Nelson, H. Hirayama, D. W. O. Rogers, SLAC-265 (Stanford University, Stanford, 1985)

[2] Y. Namito, H. Hirayama and S. Ban, "Improvements of Low-Energy Photon Transport in EGS4", In *1st International Workshop on EGS4, Japan, Aug. 26-29 1997* ed. by. H. Hirayama, Y. Namito and S. Ban, KEK Proc. **99-16**, (1997) pp.32-50

[3] Y. Namito, S. Ban and H. Hirayama, *Nucl. Instrum. and Meth. A* **332**(1993)277.

[4] Y. Namito, S. Ban and H. Hirayama, *Nucl. Instrum. and Meth. A* **349**(1994)489.

[5] H. Hirayama, Y. Namito and S. Ban, "Implementation of an L-Shell Photoelectron and an L X-ray for Elements into the EGS4 Code", *KEK Internal 96-10* (1996).

[6] Y. Namito and H. Hirayama, *Nucl. Instrum. and Meth.* **A423**(1999)238.

[7] `ftp://ftp.kek.jp/kek/kek_egs4/kek_improve/kek_improve.*`

[8] Y. Namito and H. Hirayama, "LSCAT: Low-energy Photon-scattering Expansion for the EGS4 Code (Inclusion of Electron Impact Ionization)", *KEK Internal 2000-4* (2000).

[9] H. Hirayama and Y. Namito, "General Treatment of Photoelectric Related Phenomena for Compounds and Mixtures in EGS4", *KEK Internal 2000-3* (2000).

[10] J. J. Matese and W. R. Johnson, *Phys. Rev.* **140**(1965)A1.

[11] J. M. Scofield, *At. Data and Nucl. Data Tables* **14**(1974)121.

[12] S. I. Salem and P. L. Lee, *At. Data and Nucl. Data Tables* **18**(1976)233.

[13] Y. Namito and H. Hirayama, "Improvement of the Cross-section and Branching-ratio Evaluation in EGS4 in the Energy Interval Which Has an Absorption-edge", In *8th EGS4 Users' Meeting in Japan, Japan, Aug. 1-3 1999* ed. by. H. Hirayama, Y. Namito and S. Ban, KEK Proc. **99-15**, (1999) pp.1-6.

[14] Ed C. M. Lederer V. S. Shirley, *Table of Isotopes* 7th edn (Wiley-Interscience, New York, 1978).

[15] W. Bambynek et al., *Rev. Mod. Phys.* **44**(1972)716.

[16] Ed V. S. Shirley, *Table of Isotopes* 8th edn. (Wiley-Interscience, New York, 1996).

[17] W. Bambynek, post-deadline abstract published in the Proc. of the Conference on X-ray and inner-shell processes in atoms, molecules and solids, Leipzig, Aug 20-24 (1984).

[18] N. A. Guadala et al., *Nucl. Instr. Meth. A* **347**(1994)504.

[19] H. Nakashima et al., *Nucl. Instr. Meth. A* **310**(1991)696.

[20] C. E. Dick, A. C. Lucas, J. M. Motz, R. C. Placious, J. H. Sparrow, *J. Appl. Phys.* **44**(1973)815.

[21] R. Placious, *J. Appl. Phys.* **38**(1967)2030.

[22] M. J. Berger, In *Monte Carlo transport of Electron and Photons*, eds. T. M. Jenkins, W. R. Nelson and A. Rindi (Plenum, New York, 1988) pp.216, Figure 8.27b.

[23] E. Acosta, X. Llovet, E. Coleoni, J. A. Riveros, F. Salvat, *J. Apply. Phys.* **83**(1998)6038.

[24] M. Gryziński, *Phys. Rev.* **138**, A 305, A 322, A 336 (1965).

[25] E. Casnati, A. Tartari, C. Baraldi, *J. Phys. B* **15** (1982)155

[26] E. Casnati, A. Tartari, C. Baraldi, *J. Phys. B* **16** (1983)505.

[27] L. R. M. Morin, *J. Phys. Chem. Ref. Data* **11** (1982)1091.

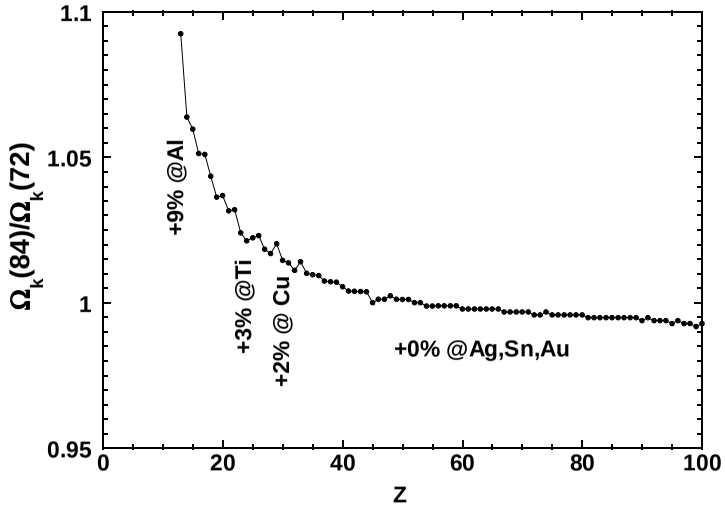

Figure 1: Ratio of currently used fluorescent yield and previously used one.

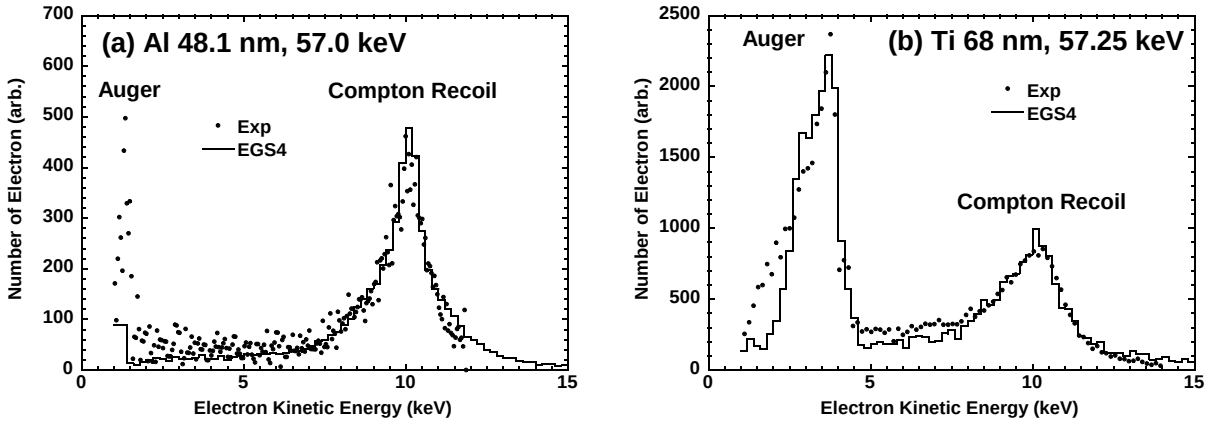

Figure 2: Comparison of the electron spectra. Incident is monochronized synchrotron radiation photon. Measurement by Guadala et al is shown by filled circles. EGS4 calculations are shown in solid line. Target materials, thickness and incident photon energies are, (a) Al 48.1 nm, 57.0 keV (b) Ti 68 nm, 57.25 keV. Incident photon energy was adjusted from Compton recoil electron energy.

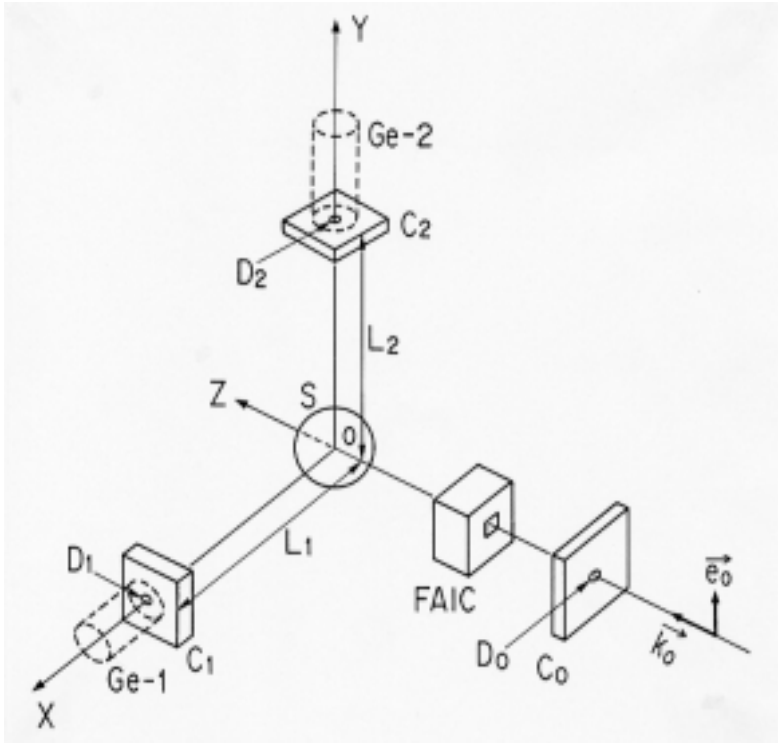

Figure 3: Experiment arrangement. A mono-energetic linearly polarized synchrotron radiation photon beam was scattered by a sample (S); the scattered photons were counted by two high-purity Ge detectors for low-energy photons (Ge_1, Ge_2). The aperture of the C_0 collimator was 2 mm. A free air ion chamber (FAIC) was located in front of the sample to monitor incident photon intensity. The sample was placed at point O; its normal vector is $(-\frac{1}{2}, -\frac{1}{\sqrt{2}}, \frac{1}{2})$. Collimators$(C_1, C_2)$ define the opening angle of Ge detectors. The distance from the surface of the sample to the exit of collimator (L_1) was 420 mm and the aperture of Collimator(D_1) was 5.01 mm.

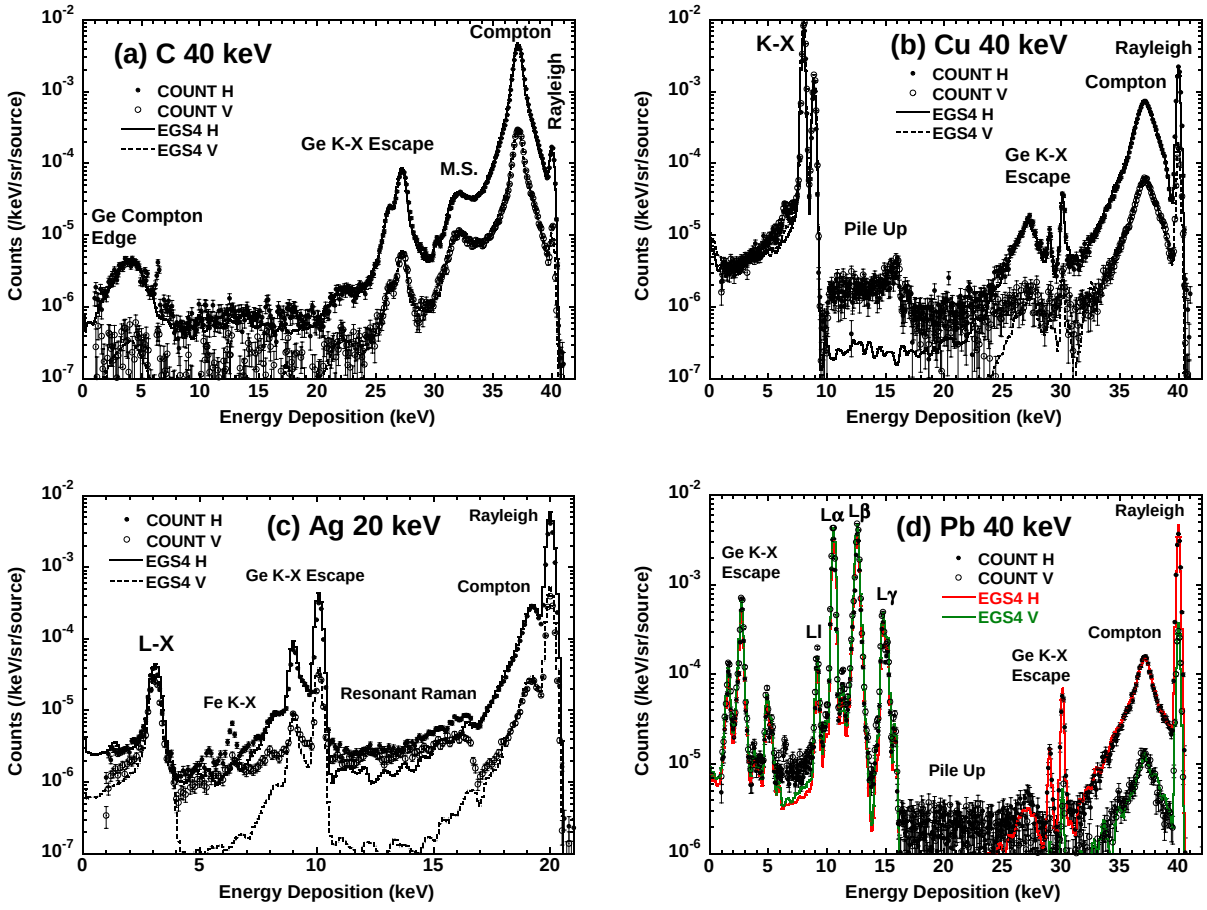

Figure 4: Comparison of the photon spectra. Measurement is shown by filled (horizontal) and open circles (vertical). EGS4 calculations are shown in solid (horizontal) and dashed (vertical). Targets and incident photon energy are, (a) C-40 keV (b) Cu-40 keV (c) Ag-20 keV (d) Pb-40 keV.

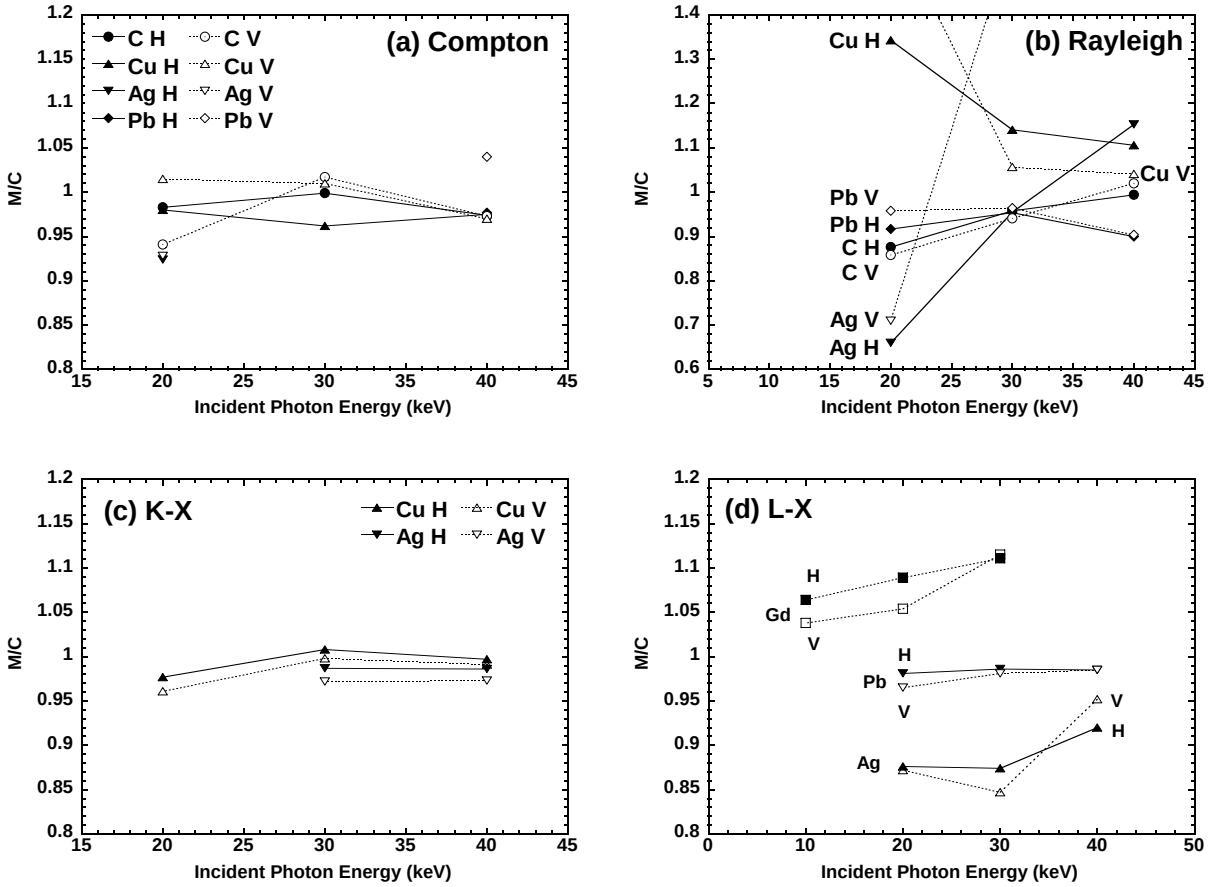

Figure 5: Ratio of measured and calculated intensity of each peak. 'H' and 'V' means horizontal and vertical respectively. (a) Compton scattering (b) Rayleigh scattering (c) K-X ray (d) L-X ray.

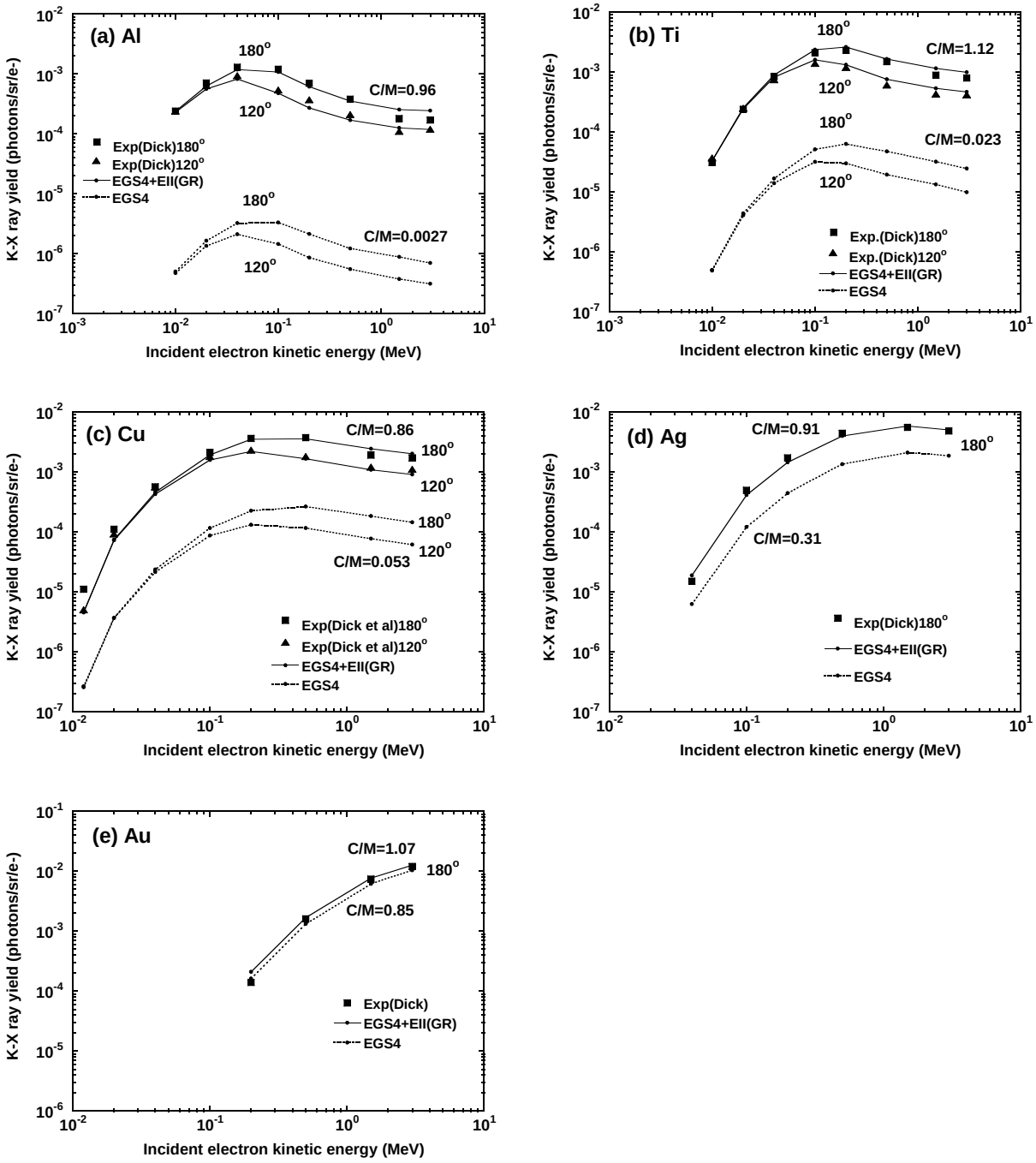

Figure 6: Comparison of the K-X ray yield. The measured values by Dick et al. are indicated by filled boxes ($\theta = 180°$) and filled triangles ($\theta = 120°$). EGS4: EGS4 calculation without EII; EGS4+EII: EGS4 calculation with EII using Gryziński's cross section. (a) Al (b) Ti (c) Cu (d) Ag (e) Au.

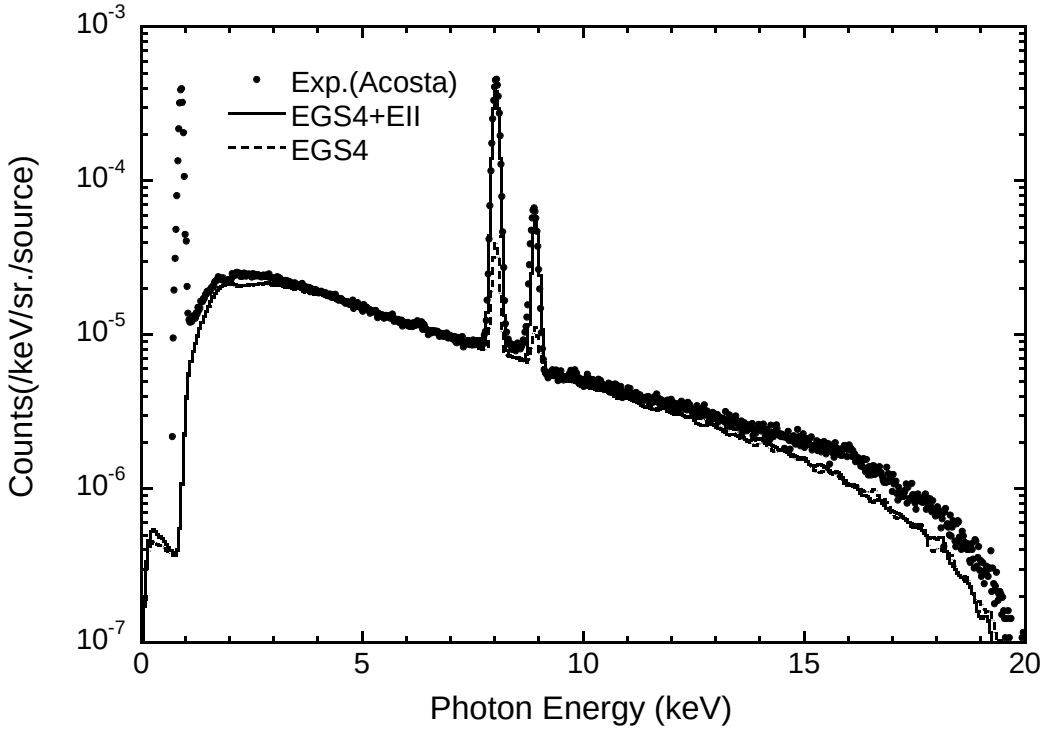

Figure 7: Spectra of the bremsstrahlung and K-X rays from a Cu target toward $\theta = 130°$. A 20 keV electron beam is normally incident on the target. The closed circle indicates a measurement using a Si detector by Acosta et al. The solid and dashed lines indicates the EGS4 calculation with EII using Gryziński's cross section and without EII.

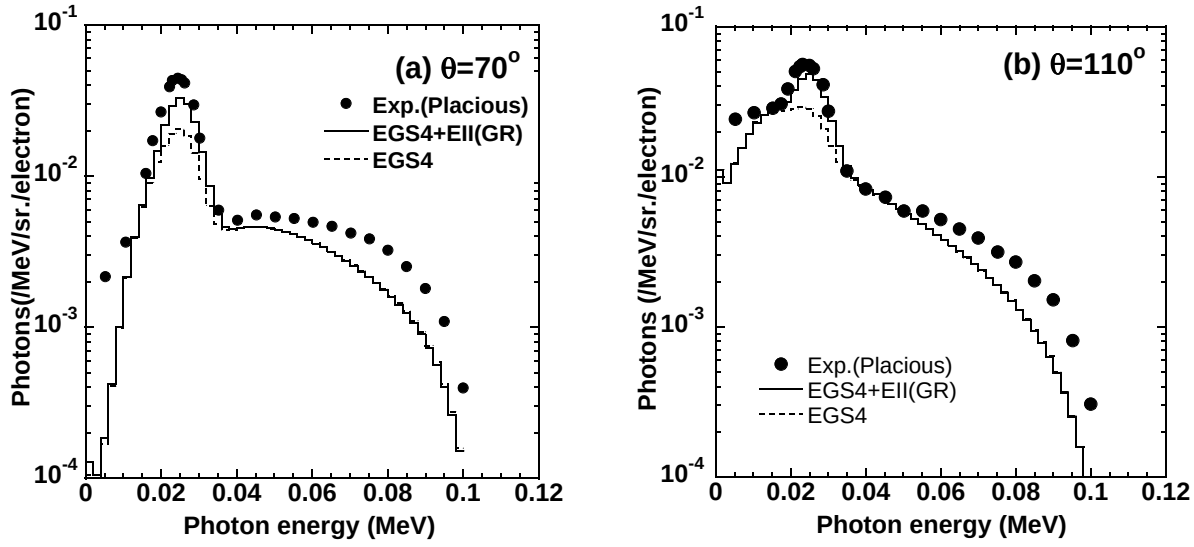

Figure 8: Spectra of the bremsstrahlung and K-X rays from a Sn target toward (a) $\theta = 70°$ and (b) $\theta = 120°$, respectively. A 100 keV electron beam is normally incident on the target. The closed circle indicates a measurement using an NaI detector by Placious. The solid and dashed lines indicates the EGS4 calculation with EII using Gryziński's cross section and without EII.